Title

Understanding the Reaction Mechanism of Lithium—Sulfur Batteries by In Situ/Operando X-ray Absorption Spectroscopy

Journal

Arabian Journal for Science and Engineering, 44(7)

ISSN

2193-567X

Authors

Zhang, Liang

Guo, Jinghua

Publication Date

2019-07-01

DOI

10.1007/s13369-019-03808-8

Peer reviewed

Understanding the Reaction Mechanism of Lithium–Sulfur Batteries by In Situ/Operando X-ray Absorption Spectroscopy

Liang Zhang[1] · Jinghua Guo[1]

Abstract

Because of the high theoretical energy density of 2600 Wh kg^{-1}, lithium–sulfur (Li–S) batteries are regarded as one of the most promising energy storage technologies to meet the increasing requirement from personal devices to automobiles. However, the practical application of Li–S batteries is still challenging due to technical obstacles, such as low sulfur utilization and poor lifetime. Therefore, understanding the electrode reaction mechanism is of critical importance to further improve the battery performance and lifetime. Here, we review recent progress in the application of in situ and operando X-ray absorption spectroscopy in characterizing Li–S batteries. We discuss in detail how this advanced technique helps researchers understand the redox process of the electrode materials as well as the influence of polymer binder and electrolyte additive on the polysulfide shuttle effect, which provide valuable information for designing better Li–S batteries. A general conclusion and critical further research directions are also provided at the end.

1 Introduction

Developing electrical energy storage systems with high energy density and low cost is vitally important for powering our future society. Lithium-ion batteries (LIBs) are one of the dominant energy storage devices at the moment, which have been widely applied in various areas, e.g., portable electronic devices and electric vehicles [1–7]. However, the specific capacities of the electrode materials for LIBs are approaching their theoretical limits, which hinders the widespread application in a variety of emerging mobile transport applications. As a consequence, new battery technologies with high energy density and low cost that go beyond conventional LIBs are highly required.

Lithium–sulfur (Li–S) batteries (Fig. 1) have attracted extensive attention in recent years due to their high theoretical capacity and specific energy compared to the existing LIBs [8–20]. For a typical Li–S battery, it consists of a lithium metal anode, an organic electrolyte and an elemental sulfur-based composite cathode. During the discharge process, the elemental sulfur is reduced first to long-chain polysulfides Li_2S_x ($4 < x \leq 8$) and then to short-chain polysulfides Li_2S_x ($2 < x \leq 4$). For devices utilizing an ether-based organic solvent, there are usually two discharge plateaus at 2.3 and 2.1 V, corresponding to the transformations of S_8 to Li_2S_4 and Li_2S_4 to Li_2S, respectively (Fig. 2). During the subsequent charge process, Li_2S is oxidized to S_8 via the formation of lithium polysulfides. Assuming a complete conversion reaction of elemental S ($16Li + S_8 \rightarrow 8Li_2S$), Li–S batteries could deliver a high specific capacity of 1675 mAh g^{-1} and specific energy of 2600 Wh kg^{-1} (Fig. 2), which are much higher than those of LIBs. Moreover, sulfur is naturally abundant and inexpensive. Therefore, Li–S batteries are considered as one of the most promising candidates for next-generation electrical energy storage systems for electric vehicles and large-area grids [8–11].

Although Li–S batteries are promising, there are still many challenges facing the Li–S technology [9,10]. For one thing, both S_8 and Li_2S are insulators with a high resistance, resulting in a low rate capability and low sulfur loading. For another thing, a volume expansion as large as 80% is expected when

✉ Jinghua Guo
jguo@lbl.gov

Liang Zhang
liangzhang@lbl.gov

[1] Advanced Light Source, Lawrence Berkeley National Laboratory, 1 Cyclotron Road, Berkeley, CA 94720, USA

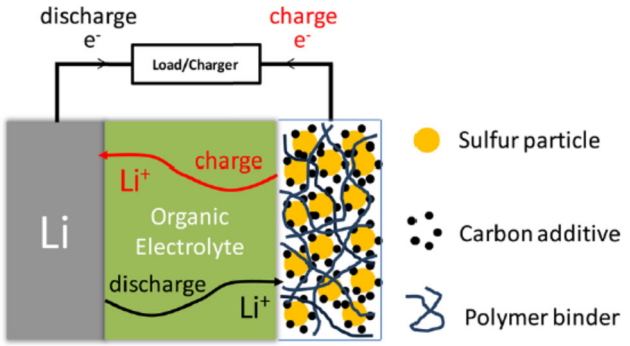

Fig. 1 Schematic diagram of a typical Li–S battery. Reproduced with permission from Ref. [10]

S_8 is fully converted to Li_2S, which leads to the pulverization of the active materials and thus rapid capacity fading. In addition, the intermediate lithium polysulfides have a high solubility in the organic electrolyte. They can diffuse toward the lithium anode to be reduced chemically and then diffuse back to the sulfur cathode to be re-oxidized, resulting in the notorious polysulfide shuttle effect.

To overcome these challenges, extensive efforts have been devoted to comprehensively understand the electrochemical reaction mechanism of Li–S batteries during the discharge–charge process to further improve the cycling performance. Among them, many studies have been focused on the complex reaction mechanism of electrode materials using advanced in situ/operando characterization techniques, such as X-ray diffraction (XRD), small-angle X-ray scattering (SAXS), Raman, neutron diffraction (ND), transmission electron microscopy (TEM) and nuclear magnetic resonance (NMR) [18,21–42]. For example, in situ/operando TEM has been applied to investigate the lithiation and volume expansion of sulfur electrodes across multiple length scales [40,41]. In addition, several groups have investigated the phase change of sulfur during cycling process using in situ/operando X-ray diffraction (XRD) [35,36]. The results indicate that the phase of sulfur obtained after charge process is different from the initial phase. Moreover, the formation of crystalline Li_2S_2 was clarified recently [43]. However, the amorphous nature of the intermediate lithium polysulfides formed during the cycling process makes it impossible to identify them with XRD.

In contrast to XRD, synchrotron-based X-ray absorption spectroscopy (XAS) is an element-specific technique and able to detect species that are amorphous, disordered or crystalline [19,44–46]. As a consequence, XAS is suitable for studying electronic and structural changes in electrode and electrolyte materials during the electrochemical processes. For soft X-ray (100–2000 eV)-based XAS, it can detect the 1s to 2p excitations of low Z elementals, such as C, N and O, and the 2p to 3d transitions of 3d transition metals, such as Mn, Fe, Co and Ni (Fig. 3a) [47]. During the XAS process, the core-level electron is excited to an unoccupied state above the Fermi level through dipole transition (Fig. 4a). The probability of such a transition is directly related to the X-ray absorption cross section.

The most straightforward measurement of the absorption process is to measure the attenuation of incident X-rays, which is the common method for hard X-ray. However, due to the short penetration depth of soft X-ray, the XAS usually collects the intensity of the decay products of core holes, i.e., auger electrons or fluorescence photons (Fig. 3b). The intensity of these secondary electrons or the photons is proportional to the X-ray absorption cross section. Because of the short mean free path of electrons, the total-electron-yield (TEY) method is very surface sensitive (typically several nm). In contrast, if the outgoing photons (total fluorescence yield, TFY) are detected, the XAS becomes bulk sensitive (several hundred nm to μm, depending on the X-ray energy) due to the comparatively larger attenuation length. It should be noticed that both TEY and TFY modes are based on secondary X-ray excitation and relaxation processes. The TEY mode is usually measured by the sample drain current and therefore is limited to conductive materials, while TFY mode may be distorted by the saturation effect resulting from the

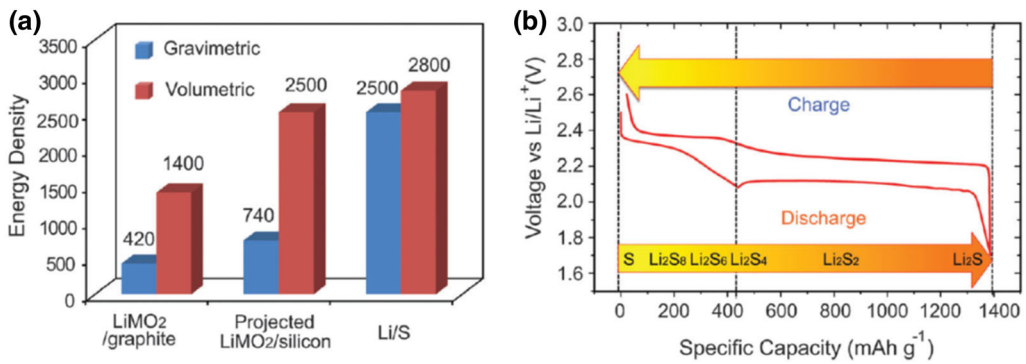

Fig. 2 **a** Energy density of Li–S batteries compared with other batteries. **b** A typical discharge/charge voltage profile of Li–S batteries in ether-based electrolytes. Reproduced with permission from Refs. [8] and [10]

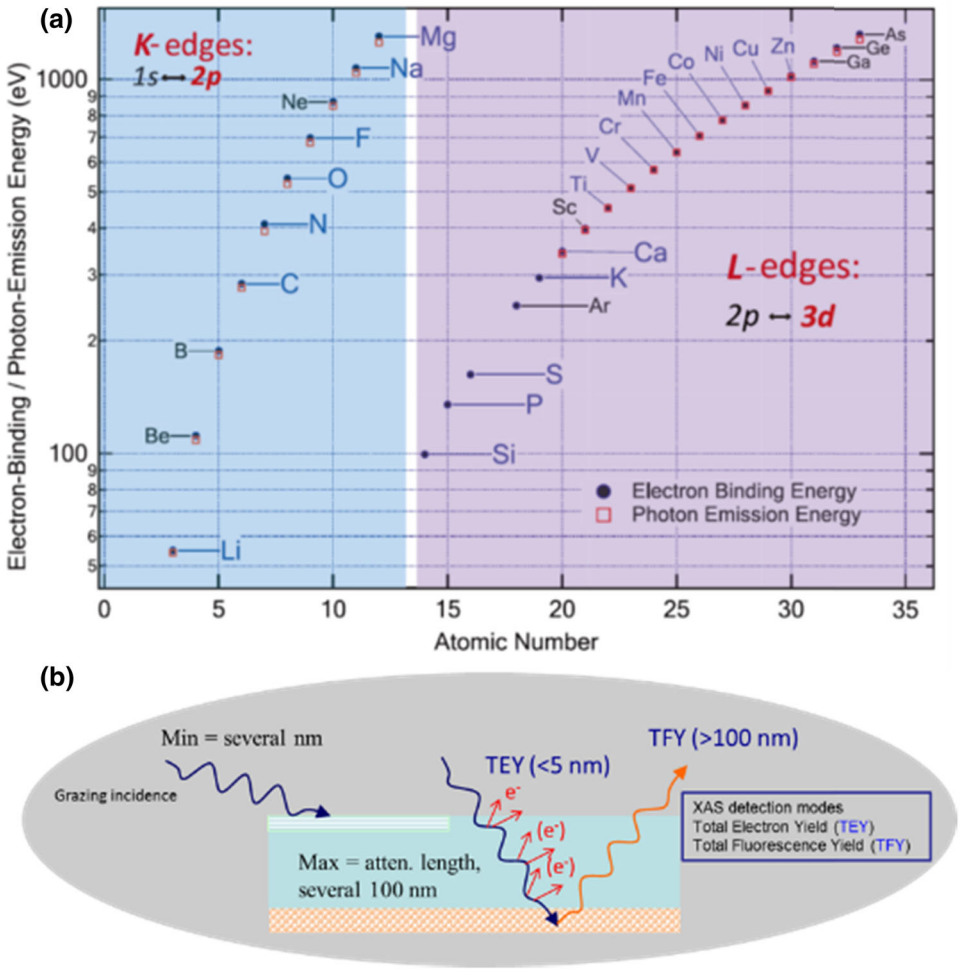

Fig. 3 **a** Elements and corresponding excitations that are accessible by soft XAS. Reproduced with permission from Ref. [44]. **b** The geometry of XAS detection

self-absorption effect. For example, by measuring C and O K-edge XAS (Fig. 3b, c), we have investigated the chemical interaction between sulfur and graphene oxide (GO). The results clearly indicate that the moderate chemical interaction between GO and sulfur can not only preserve the intrinsic electronic structure of GO but also confine the sulfur on GO sheets, which can greatly improve the cycling performance of Li–S batteries [48,49]. In addition, XAS is a powerful tool in resolving electronic structures and distinguishing different electronic states, such as the different oxidation states and spin states of different Ni species shown in Fig. 3d [50]. For S K-edge XAS spectra, different sulfur species, e.g., elemental sulfur, Li_2S and lithium polysulfides, can be clearly distinguished [22–24,51].

While most of the reported reviews have summarized the recent progress on structural design of different components (e.g., sulfur electrodes, separators, electrolytes and anodes) and performance improvement of Li–S batteries [8–10,12,13,52–54], only a few reviews focus on the fundamental understanding of the reaction mechanism [19,55]. Synchrotron-based characterization techniques (especially XAS) have been widely used to investigate the reaction mechanism of Li–S batteries. Specially, significant progress has been achieved by using in situ/operando XAS to understand the redox process of electrode materials for Li–S batteries. In this contribution, we review recent progress in advanced characterization of Li–S batteries using in situ and operando XAS through four aspects: (1) the redox mechanism of S electrode; (2) the redox mechanism of Li_2S electrode; (3) the influence of polymer binder on the polysulfide shuttle effect; and (4) the influence of electrolyte additive on the polysulfide shuttle effect. In addition, we also provide perspectives on how the in situ and operando XAS can contribute to the further development of high-performance Li–S batteries.

2 Redox Mechanism of S Electrode

For a typical Li–S battery, elemental sulfur S_8-based composite materials are usually used as the cathode materials. During the past few years, the redox mechanism of S_8 has been extensively investigated for Li–S batteries under the working conditions by using in situ/operando XAS. For example, Cuisinier et al. investigated the sulfur speciation during

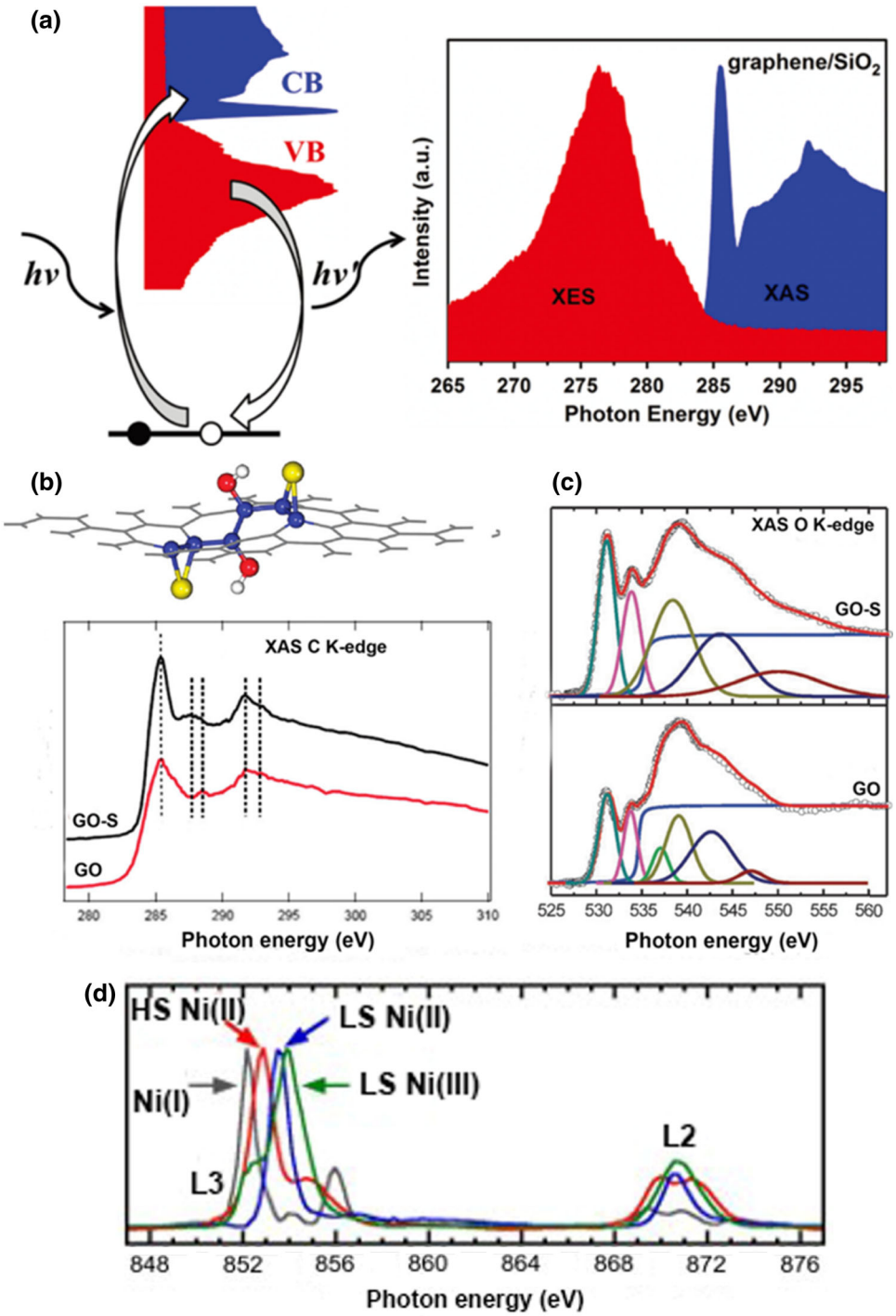

Fig. 4 **a** Schematic illustration of the X-ray absorption and emission processes. **b** Representative pattern of GO immobilizing S and C K-edge XAS spectra of GO and GO-S. **c** O K-edge XAS spectra of GO and GO-S. **d** The Ni L-edge XAS spectra of different Ni-related species. Reproduced with permission from Refs. [45–47]

redox behavior and the mechanisms that control the dissolution and deposition of the redox products (S_8 and Li_2S) using in situ/operando XAS with a focus on S K-edge with low dielectric solvents 1,3-dioxolane-1,2-dimethoxyethane (DOL–DME), as shown in Fig. 5 [33]. To avoid the potential distortion of the XAS spectra by bulk particles, they used extremely uniform porous carbon nanospheres (PCNS, with a controlled size of 220 nm)/S composites as the cathode electrode. This unique composition can not only confine the active electrode materials within the cathode side and therefore improve the cycling performance, but also facilitate the in situ/operando investigation. By using a linear combination of the operando XAS spectra, it is revealed that owing to the supersaturation of S^{2-} the precipitation of Li_2S is delayed during discharge, while the surface oxidization of Li_2S proceeds straightforwardly with the formation of intermediate

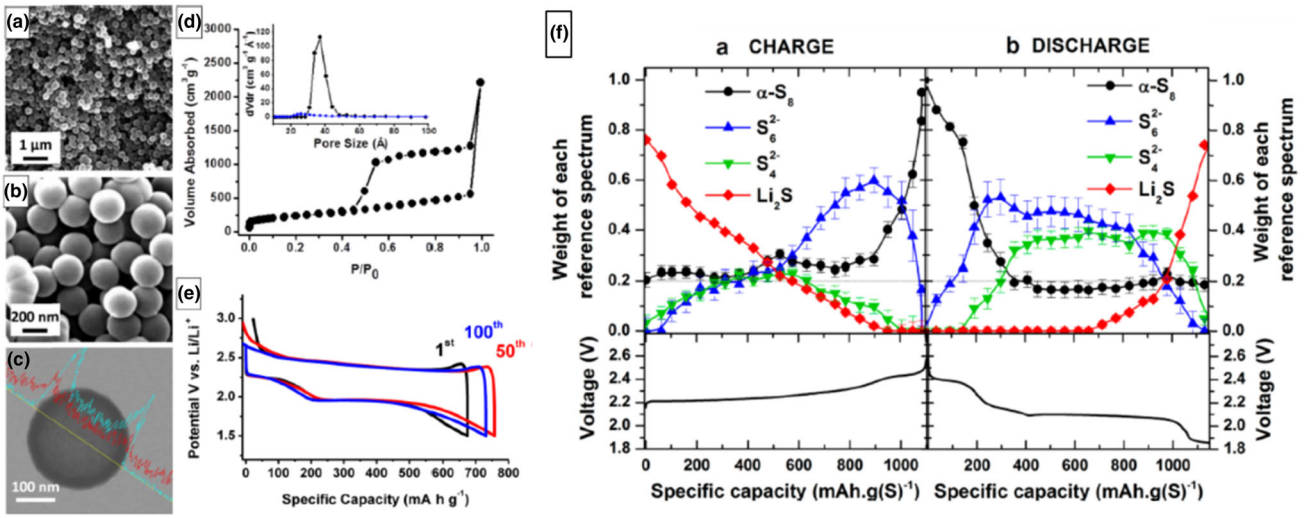

Fig. 5 **a**–**c** SEM images and EDX line of synthesized porous carbon nanospheres for S cathode. **d** Pore size distribution of porous carbon nanospheres with and without sulfur. **e** The discharge–charge voltages for the first, 50th and 100th cycles. **f** Evolution of sulfur K-edge XAS spectra upon electrochemical cycling based on linear combination analysis. Reproduced with permission from Ref. [33]

lithium polysulfides, i.e., Li_2S_4 and Li_2S_6. The XAS results also indicate that the discharge capacity is not limited by the precipitation of Li_2S but restricted by the unreacted sulfur [33].

By changing the solvents from low dielectric DOL–DME to high dielectric dimethylacetamide (DMA), the Li–S batteries undergo a series of electrochemical and chemical reactions with the intermediate reaction products of S_8^{2-}, S_6^{2-}, S_4^{2-} and $S_3^{\bullet-}$, among which $S_3^{\bullet-}$ is the most stable and dominant intermediate species [56]. In addition, Vijayakumar et al. stated that $S_3^{\bullet-}$ is the only free radical anion shown in the dimethyl sulfoxide (DMSO) solvent [57]. Actually, $S_3^{\bullet-}$ is also the only radical anion for a sulfur electrode discharged in tetraethylene glycol dimethyl ether (TEGDME) [58]. Moreover, Wujcik et al. found that significant quantities of polysulfide radical species (LiS_3, LiS_4, and LiS_5) are present after initial discharge to 2.0 V for Li–S batteries using ether-based solvents, while increased concentrations of shorter polysulfide dianions are observed after further discharge to 1.8 V [51]. By using a specifically designed electrochemical cell, Gorlin et al. investigated the influence of the solvent (DOL–DME vs. DMA) on the conversion of polysulfides to Li_2S by using in situ/operando XAS [24]. The results clearly demonstrate the formation of Li_2S after $\sim$ 25–30% discharge in both types of solvents. However, the subsequent conversion from polysulfides to Li_2S is more rapid in DOL–DME. At the end of charge, the presence of Li_2S and lithium polysulfides is observed for DMC cells, while a mixture of Li_2S and S_2^{2-}/Li_2S_2 like intermediate is observed for cells using DOL–DME. All these results clearly indicate that the intermediate polysulfide species are highly related to the choice of the solvent. Overall, the in situ/operando XAS has provided invaluable insights toward a clear understanding of the redox mechanism of sulfur electrodes in Li–S batteries under real operation conditions, which is essential for further optimizing and improving the cycling performances.

3 Redox Mechanism of Li_2S Electrode

Besides the sulfur electrode, the Li_2S electrode (theoretical capacity: 1166 mAh g^{-1}) also attracts extensive attention because it can be paired with not only lithium but also other much safer anodes (such as graphite, silicon and tin), which can obviate the safety issues of the lithium metal anode when using sulfur [59–67]. In addition, compared with the low melting point of sulfur (115 °C), Li_2S has a much higher melting point (1372 °C), which guarantees the application of high-temperature heat treatment of Li_2S to protect the electrode materials and prevent the dissolution of lithium polysulfides into the electrolyte. Moreover, the mechanical damage of the cathode during the cycling process can also be circumvented because Li_2S is in the maximal volume and the empty space generated during the charge process therefore can hold the volume expansion of sulfur during the discharge process.

The electrochemical performance of Li_2S has been investigated in detail previously. For example, Yang et al. found that a large overpotential barrier ($\sim$ 1V) exists for micrometer-sized Li_2S particles [65]. The initial potential barrier can be overcome by applying a high charging cut-off voltage. During the activation process, polysulfide phase can be formed, which greatly improves the kinetics of Li_2S.

The Li_2S particles with an average side of 10 μm can also be activated by using this method, and a high discharge capacity of 850 mAh/g is achieved [65]. The activation mechanism was also investigated by using in situ X-ray diffraction. The results indicate that the origin of the initial barrier is a result of phase nucleation, while the height of the barrier is mainly related to the poor charge transfer at the surface of Li_2S and limited diffusivity of lithium ions inside Li_2S. Cai et al. further improved the cycling performance of Li_2S electrode by using a cost-effective way preparing nanostructured Li_2S-carbon composite using high-energy dry ball milling of commercial Li_2S powder [61]. More recently, Nan et al. reported an easy synthesis strategy for the preparation of Li_2S spheres with controlled size and a chemical vapor deposition (CVD) method for coating Li_2S spheres with a carbon shell, which is porous enough to allow Li^+ diffusion in and out of the core–shell particles [60]. The unique core–shell particles deliver both high specific capacity and stable cycling performance.

For all the reported results, an activation process is always necessary to make full utilization of the Li_2S electrode materials [60]. To understand this abnormal behavior, the charging mechanism of Li_2S electrode has been extensively investigated [22,23,30,60,63,66,68]. For instance, by using spatially resolved XAS characterization, which can detect lithium polysulfides in the electrolytic solutions and amorphous/crystalline solids and differentiate between species formed in the electrode and the electrolytic solutions, Gorlin et al. investigated the intermediate products formed in the cathode and electrolytic solutions during the first and second charge processes to gain insight into the Li_2S redox mechanism in the DOL–DME solvent [22]. The results indicate that the first charge process leads to a complete conversion of Li_2S to S_8 with no significant concentration of intermediate polysulfides detected throughout the whole process. The oxidation of Li_2S particles also requires a chemical step, which is facilitated by the presence of a significant concentration of intermediate polysulfides.

However, the reason for the presence of the energy barrier was not explained in that report. To answer this question, we have investigated the electrochemical charging mechanism of nanosized Li_2S with a uniform size of $\sim$ 500 nm by in situ/operando XAS [23]. As shown in Fig. 6, the characteristic XAS features of different sulfur species can be well discerned in the XAS spectra. The in situ/operando XAS results indicate that in the first charge process, Li_2S is directly converted to S without the formation of lithium polysulfides, while the formation of lithium polysulfides is visible from the beginning of the second charge process (Fig. 6). As a consequence, a high charging voltage is always essential to fully extract Li^+ from Li_2S into electrolyte in the first charge process considering the fact that Li_2S is an ionic crystal. The presence of lithium polysulfides at the beginning of the second charge process has multiple effects: (1) reducing the charge transfer resistance from Li_2S to electrolyte and leading to a lower overpotential in the charge voltage profile; (2) acting as the polysulfide facilitator for the electrochemical reaction of Li_2S; and (3) reacting chemically with Li_2S to form low-order polysulfides. This investigation provides a new fundamental insight into the charge mechanism of the Li_2S electrode and highlights the double roles of the lithium polysulfides in both the electrochemical and chemical processes. It should be noted that Li_2S is most likely amorphous after the first cycle, as revealed by in situ/operando high-energy XRD [69].

4 Effect of Polymer Binder for Polysulfide Shuttle Effect

As mentioned above, the soluble nature of lithium polysulfides results in the shuttle effect for Li–S batteries, which is harmful for the electrochemical performance. Tremendous efforts have been taken to solve this problem, such as integrating sulfur with porous carbon, graphene and graphene oxide [48,49,70–74]. The physical trap of sulfur is effective for improving the electronic conductivity and suppressing the shuttle effect. An alternative route is to modify the functional polymer binders for Li–S batteries, which play a role of gluing the elemental sulfur and conductive additives together. Polyvinylidene fluoride (PVDF) is a conventional binder for Li–S batteries, but lacks chemical bonding with intermediate lithium polysulfides that are formed during the discharge and charge processes.

As a consequence, different functional polymer binders have been developed to improve the cycling performance of Li–S batteries [75–80]. For example, by applying a new amino-based functional binder with 3D network flexibility structure, the capacity is still retained at 91.3% over 600 cycles [76]. In addition, a high specific capacity of 987.6 mAh g^{-1} is achieved with a high sulfur loading density of 8.0 mg cm^{-2}. According to the in situ UV–Vis absorption spectra analysis, the origin responsible for the enhanced electrochemical performance is related to the abundant amino groups of the binder with high binding strength to lithium polysulfides, which could effectively reduce the polysulfide dissolution and therefore the shuttle effect [76]. This also spurred the investigation into natural polymers as multifunctional binders for Li–S batteries to suppress the shuttle effect. For example, gum Arabic, a bio-derived polymer with abundant functional groups, has been successfully applied to Li–S batteries, resulting in an outstanding performance and stability over 500 cycles [81]. Recently, we demonstrated that there exists an nucleophilic substitution reaction between lithium polysulfides and carrageenan polymer binder, which can fix the lithium polysulfides to the

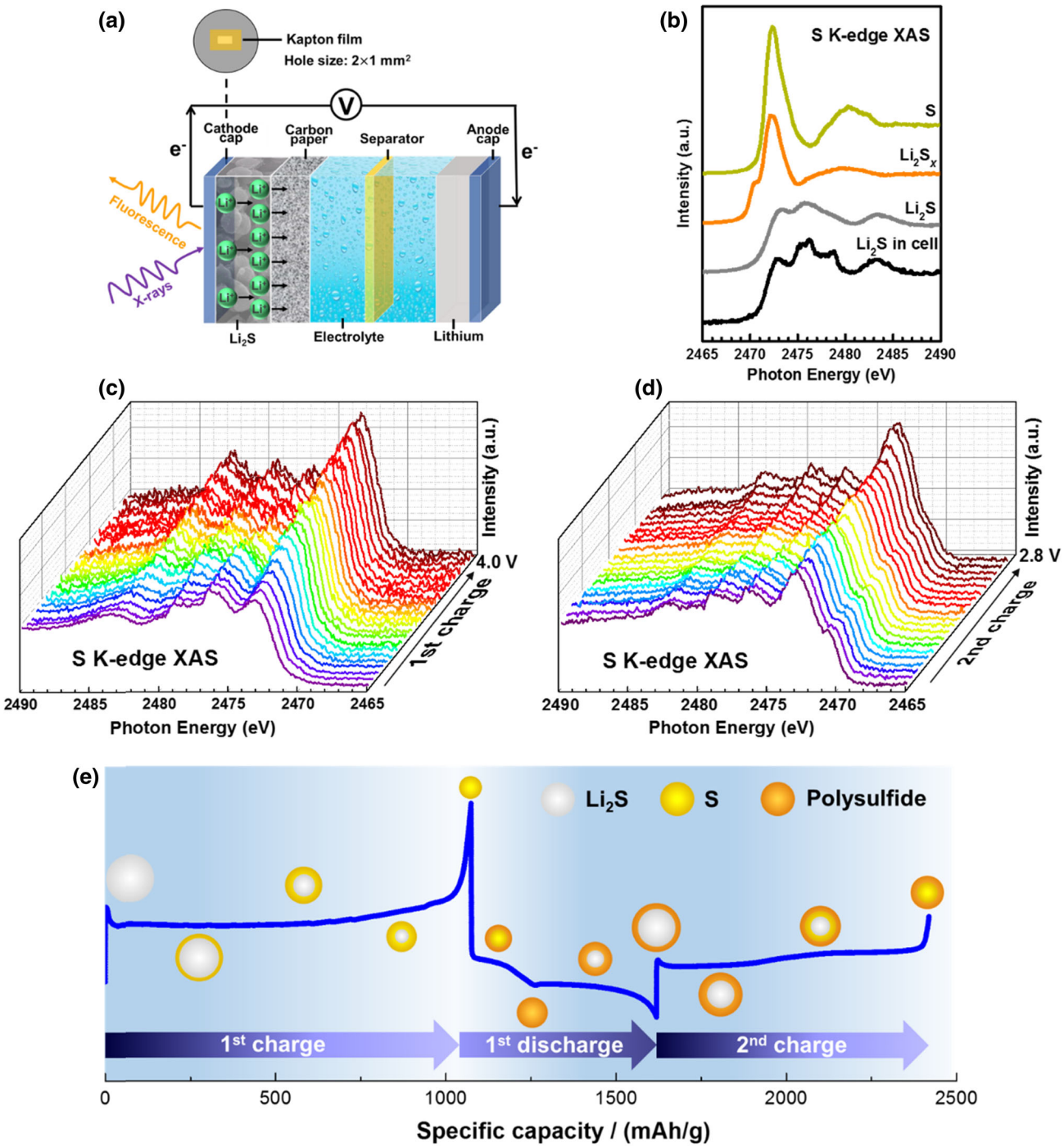

Fig. 6 Reaction mechanism of Li_2S electrode by in situ and operando XAS. **a** Schematic illustration of the in situ coin cell for simultaneous electrochemical and X-ray spectroscopic measurement. **b** S K-edge XAS of different sulfur species. **c** Operando XAS spectra of Li_2S electrode for the first charge process. **d** Operando XAS spectra of Li_2S electrode for the second charge process. **e** The proposed reaction mechanism of Li2S electrode during the initial charge and discharge processes. Reproduced with permission from Ref. [23]

sulfur electrode via the newly formed C–S covalent bond [82]. These polymer binders can continuously react with the polysulfides when they break from the electrode during the cycling process. In addition, we showed that the polyethylenimine (PEI) polymer can be applied as a polar binder for Li–S batteries to hinder the shuttle effect [83]. The sulfur electrode (8.6 mg cm^{-2}) with PEI binder can deliver a high initial areal capacity of 9.7 mAh cm^{-2}, and

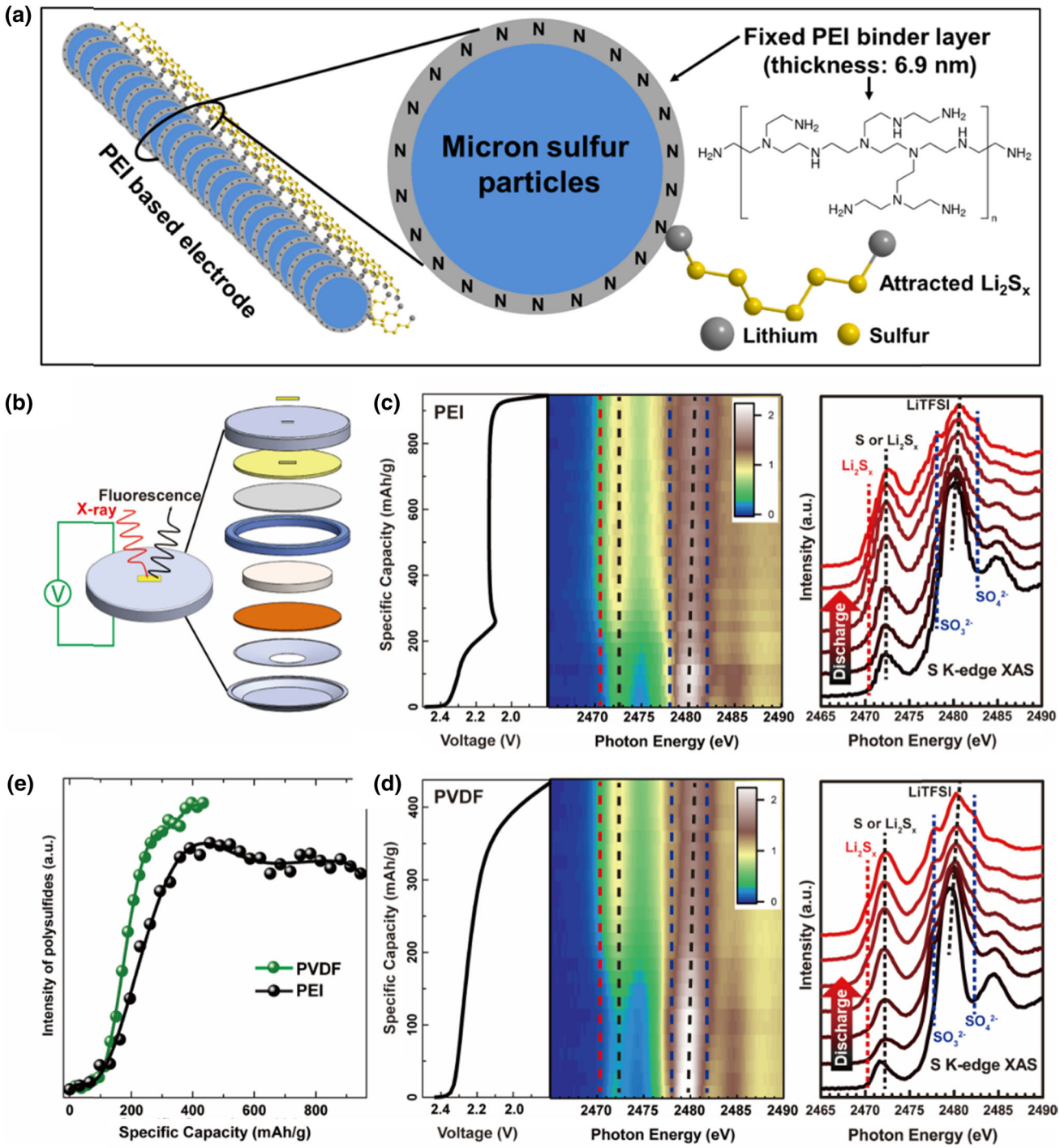

Fig. 7 Effect of polymer binder for polysulfide shuttle effect. **a** Schematic illustration of the lithium polysulfide confinement through PEI polymer binder. **b** Cell configuration for operando XAS study. **c** Operando sulfur K-edge XAS mapping and representative XAS spectra of PEI-based cathode during first discharge. **d** Operando sulfur K-edge XAS mapping and representative XAS spectra of PVDF-based cathode during first discharge. **e** Concentration of polysulfides in electrolyte for PEI- and PVDF-based cathodes as a function of specific capacity during first discharge. Reproduced with permission from Ref. [83]

the capacity is still maintained at 6.4 mAh cm^{-2} after 50 cycles, which is comparable to that of commercial LIBs. The in situ UV–Vis and in situ/operando XAS spectra clearly show the strong adsorption capability of PEI binder toward lithium polysulfides because of the electrostatic interaction, which is responsible for the superior cycling performance (Fig. 7) [83].

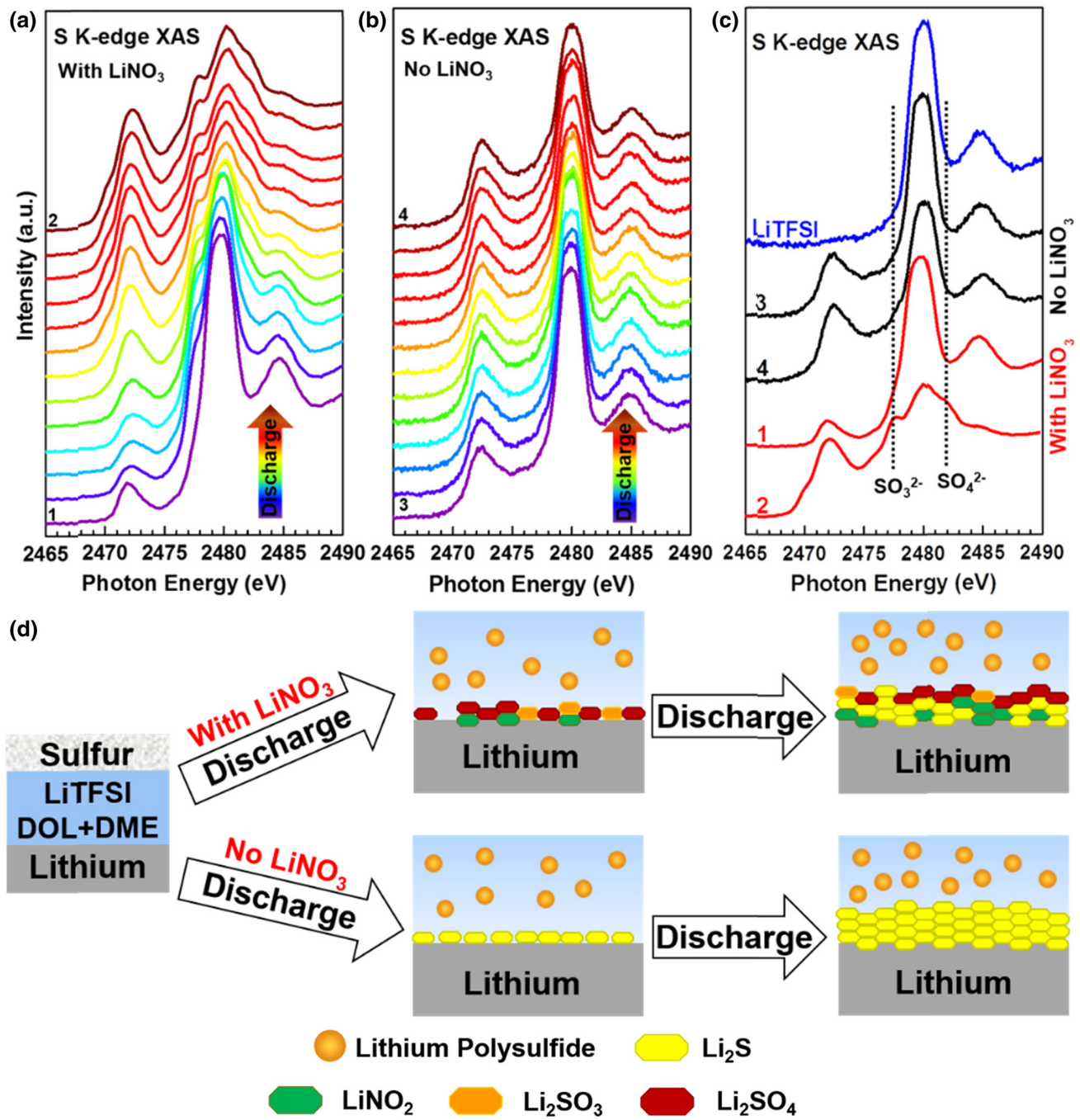

Fig. 8 Effect of $LiNO_3$ additive for polysulfide shuttle effect. In situ/operando S K-edge XAS spectra of Li–S batteries with (**a**) and without (**b**) $LiNO_3$ additive collected for the first discharge. **c** S K-edge XAS spectra of Li–S batteries at different states of charge. **d** The proposed reaction mechanism of the SEI layer. Reproduced with permission from Ref. [25]

5 Effect of Electrolyte Additive for Polysulfide Shuttle Effect

$LiNO_3$ has been widely applied as an electrolyte additive in Li–S batteries for suppressing the polysulfide shuttle effect [84–95]. It has been reported that $LiNO_3$ can participate in the formation of solid electrolyte interphase (SEI) layer on the surface of lithium anode [86,88]. The passivation film formed with $LiNO_3$ can not only protect lithium anode from chemical reaction with the dissolved lithium polysulfides but also prevent lithium polysulfides from electrochemical reduction on the lithium anode surface [86]. The reaction product of

$LiNO_3$ as well as the influence on the formation of SEI layer has been investigated extensively. For example, Xiong et al. investigated the structure of SEI layer formed in the electrolytic solution with mixed lithium salts and additives ($LiNO_3$ and lithium polysulfides) using X-ray photoelectron spectroscopy and argon-ion sputtering technology [91]. It is found that the thin SEI layer is mainly composed of two sub-layers: The top layer is mainly composed of oxidized polysulfide products while the bottom layer is formed by the reduced polysulfide and $LiNO_3$ products [91]. The unique SEI film results in a smooth and compact layer, which can effectively hinder the continuous reaction with lithium anode. In addition, the $LiNO_3$ additive can also inhibit the gassing of Li–S batteries [96]. CH_4 and H_2 are found as the major gaseous decomposition products for the operating Li–S batteries, especially during the charge process when a fresh lithium surface is created. When adding $LiNO_3$ in the electrolyte, the formation of CH_4 is greatly suppressed and very little or no H_2 is generated during discharge process. This phenomenon is possibly related to the formation of a relatively stable SEI layer on lithium surface and the suppression of polysulfide shuttle effect. Moreover, it seems that the produced gases are also consumed during the cycling process and possibly buried in the SEI layer. In addition, the concentration of dissolved lithium polysulfides can also influence the performance of $LiNO_3$ additive. If it is too high, the formed SEI layer is not well maintained and the lithium metal is easily etched, resulting in the growth of lithium dendrites and lower cycling efficiency [97].

More recently, we have comprehensively investigated the influence of $LiNO_3$ additive on the formation mechanism of the SEI layer on lithium anode surface using in situ/operando XAS (Fig. 8) [25]. The results imply that the improved cycling performance of Li–S batteries using $LiNO_3$ additive is related to the synergetic effect of $LiNO_3$ and dissolved lithium polysulfides in the electrolytic solutions. The $LiNO_3$ additive oxidizes the lithium polysulfides while itself is reduced to $LiNO_2$. The oxidization products Li_2SO_3 and Li_2SO_4 form a compact and stable layer on lithium anode surface during the initial discharge stage. This passivation layer can inhibit the reaction between lithium polysulfides and lithium metal, leading to the decrease of the shuttle effect and improvement in the cycling performance. This study therefore provides a deeper insight into the role of $LiNO_3$ for ameliorating the shuttle effect, which is important for the further development of high-performance Li–S batteries.

6 Conclusions

To summarize, we have summarized recent progress on the application of in situ/operando XAS in the understanding of the redox mechanism of Li–S batteries, which is of great significance for the development of high-performance Li–S batteries. The new insights that the in situ/operando XAS results have offered contribute to a real-time monitoring on the electronic structure evolution of both cathode and anode materials for Li–S batteries. With the aid of in situ/operando XAS, the reaction mechanism of sulfur and Li_2S electrodes has been clearly revealed. In addition, the confinement of intermediate lithium polysulfides formed during the discharge and charge processes by functional polymer binders has been visualized in detail by the same method. Moreover, the synergetic effect of $LiNO_3$ and lithium polysulfides on the formation process of the SEI layer on lithium anode and polysulfide shuttle effect are also well understood.

Although significant progress has been achieved by using in situ/operando XAS for Li–S batteries, there are still quite some questions to be answered. For example, how are the single sulfur and Li_2S particle discharged and charged during the cycling process? What is the reaction path of sulfur and Li_2S electrode during the fast discharge and charge process? Why the concentration of lithium polysulfides in the electrolyte can influence the passivation behavior of lithium anode? To answer these questions, time- and space-resolved in situ/operando XAS combined with other characterization techniques is highly required. With the recent development of diffraction-limited storage ring technique [98,99], the X-ray nanoprobe method with high beam flux and brilliance is highly promising, which can be greatly beneficial for better understanding of the reaction mechanism of Li–S batteries in the future.

Acknowledgements The work at the Advanced Light Source of the Lawrence Berkeley National Laboratory was supported by the director, Office of Science, Office of Basic Energy Sciences, of the US Department of Energy under Contract No. DE-AC02-05CH11231. This work was supported as part of the Joint Center for Energy Storage Research, an Energy Innovation Hub funded by the US Department of Energy, Office of Science, Basic Energy Sciences.

References

1. Xu, K.: Electrolytes and interphases in Li–ion batteries and beyond. Chem. Rev. **114**, 11503–618 (2014)
2. Armand, M.; Tarascon, J.-M.: Building better batteries. Nature **451**, 652–657 (2008)
3. Li, M.; Lu, J.; Chen, Z.; Amine, K.: 30 years of lithium–ion batteries. Adv. Mater. **30**, 1800561 (2018)
4. Chu, S.; Cui, Y.; Liu, N.: The path towards sustainable energy. Nat. Mater. **16**, 16–22 (2016)
5. Meng, J.; Guo, H.; Niu, C.; Zhao, Y.; Xu, L.; Li, Q.; Mai, L.: Advances in structure and property optimizations of battery electrode materials. Joule **1**, 522 (2017)
6. Lin, D.; Liu, Y.; Cui, Y.: Reviving the lithium metal anode for high-energy batteries. Nat. Nanotechnol. **12**, 194–206 (2017)
7. Nitta, N.; Wu, F.; Lee, J.T.; Yushin, G.: Li–ion battery materials: present and future. Mater. Today **18**, 252–264 (2015)

8. Yang, Y.; Zheng, G.; Cui, Y.: Nanostructured sulfur cathodes. Chem. Soc. Rev. **42**, 3018–32 (2013)
9. Seh, Z.W.; Sun, Y.; Zhang, Q.; Cui, Y.: Designing high-energy lithium–sulfur batteries. Chem. Soc. Rev. **45**, 5605–5634 (2016)
10. Manthiram, A.; Fu, Y.; Chung, S.H.; Zu, C.; Su, Y.S.: Rechargeable lithium–sulfur batteries. Chem. Rev. **114**, 11751–87 (2014)
11. Pang, Q.; Liang, X.; Kwok, C.Y.; Nazar, L.F.: Advances in lithium–sulfur batteries based on multifunctional cathodes and electrolytes. Nat. Energy **1**, 16132 (2016)
12. Fang, R.; Zhao, S.; Sun, Z.; Wang, D.W.; Cheng, H.M.; Li, F.: More reliable lithium–sulfur batteries: status solutions and prospects. Adv. Mater. **29**, 1606823 (2017)
13. Li, G.; Wang, S.; Zhang, Y.; Li, M.; Chen, Z.; Lu, J.: Revisiting the role of polysulfides in lithium–sulfur batteries. Adv. Mater. **30**, 1705590 (2018)
14. Rosenman, A.; Markevich, E.; Salitra, G.; Aurbach, D.; Garsuch, A.; Chesneau, F.F.: Review on Li–sulfur battery systems: an integral perspective. Adv. Energy Mater. **5**, 1500212 (2015)
15. Urbonaite, S.; Poux, T.; Novák, P.: Progress towards commercially viable Li–S battery cells. Adv. Energy Mater. **5**, 1500118 (2015)
16. Wang, H.; Adams, B.D.; Pan, H.; Zhang, L.; Han, K.S.; Estevez, L.; Lu, D.; Jia, H.; Feng, J.; Guo, J.; Zavadil, K.R.; Shao, Y.; Zhang, J.-G.: Tailored reaction route by micropore confinement for Li–S batteries operating under lean electrolyte conditions. Adv. Energy Mater. **8**, 1800590 (2018)
17. Ji, X.; Lee, K.T.; Nazar, L.F.: A highly ordered nanostructured carbon–sulphur cathode for lithium–sulphur batteries. Nat. Mater. **8**, 500–6 (2009)
18. Bruce, P.G.; Freunberger, S.A.; Hardwick, L.J.; Tarascon, J.M.: $Li–O_2$ and Li–S batteries with high energy storage. Nat. Mater. **11**, 19–29 (2012)
19. Zhao, E.; Nie, K.; Yu, X.; Hu, Y.-S.; Wang, F.; Xiao, J.; Li, H.; Huang, X.: Advanced characterization techniques in promoting mechanism understanding for lithium–sulfur batteries. Adv. Funct. Mater. **28**, 1707543 (2018)
20. Chen, L.; Shaw, L.L.: Recent advances in lithium–sulfur batteries. J. Power Sources **267**, 770–783 (2014)
21. Liu, Y.; He, P.; Zhou, H.: Rechargeable solid-state Li–air and Li–S batteries: materials, construction, and challenges. Adv. Energy Mater. **8**, 1701602 (2018)
22. Gorlin, Y.; Patel, M.U.M.; Freiberg, A.; He, Q.; Piana, M.; Tromp, M.; Gasteiger, H.A.: Understanding the charging mechanism of lithium–sulfur batteries using spatially resolved operando X-ray absorption spectroscopy. J. Electrochem. Soc. **163**, A930–A939 (2016)
23. Zhang, L.; Sun, D.; Feng, J.; Cairns, E.J.; Guo, J.: Revealing the electrochemical charging mechanism of nanosized Li_2S by in situ and operando X-ray absorption spectroscopy. Nano Lett. **17**, 5084–5091 (2017)
24. Gorlin, Y.; Siebel, A.; Piana, M.; Huthwelker, T.; Jha, H.; Monsch, G.; Kraus, F.; Gasteiger, H.A.; Tromp, M.: Operando characterization of intermediates produced in a lithium–sulfur battery. J. Electrochem. Soc. **162**, A1146–A1155 (2015)
25. Zhang, L.; Ling, M.; Feng, J.; Mai, L.; Liu, G.; Guo, J.: The synergetic interaction between $LiNO_3$ and lithium polysulfides for suppressing shuttle effect of lithium–sulfur batteries. Energy Storage Mater. **11**, 24 (2018)
26. Zhu, W.; Paolella, A.; Kim, C.S.; Liu, D.; Feng, Z.; Gagnon, C.; Trottier, J.; Vijh, A.; Guerfi, A.; Mauger, A.; Julien, C.M.; Armand, M.; Zaghib, K.: Investigation of the reaction mechanism of lithium sulfur batteries in different electrolyte systems by in situ Raman spectroscopy and in situ X-ray diffraction. Sustain. Energy Fuels **1**, 737–747 (2017)
27. Saqib, N.; Ohlhausen, G.M.; Porter, J.M.: In operando infrared spectroscopy of lithium polysulfides using a novel spectro-electrochemical cell. J. Power Sources **364**, 266–271 (2017)
28. Sun, Y.; Seh, Z.W.; Li, W.; Yao, H.; Zheng, G.; Cui, Y.: In-operando optical imaging of temporal and spatial distribution of polysulfides in lithium–sulfur batteries. Nano Energy **11**, 579–586 (2015)
29. Patel, M.U.; Arcon, I.; Aquilanti, G.; Stievano, L.; Mali, G.; Dominko, R.: X-ray absorption near-edge structure and nuclear magnetic resonance study of the lithium–sulfur battery and its components. Chemphyschem **15**, 894–904 (2014)
30. Vizintin, A.; Chabanne, L.; Tchernychova, E.; Arčon, I.; Stievano, L.; Aquilanti, G.; Antonietti, M.; Fellinger, T.-P.; Dominko, R.: The mechanism of Li_2S activation in lithium–sulfur batteries: can we avoid the polysulfide formation? J. Power Sources **344**, 208–217 (2017)
31. Dominko, R.; Patel, M.U.M.; Lapornik, V.; Vizintin, A.; Koželj, M.; Tušar, N.N.; Arčon, I.; Stievano, L.; Aquilanti, G.: Analytical detection of polysulfides in the presence of adsorption additives by operando X-ray absorption spectroscopy. J. Phys. Cem. C **119**, 19001–19010 (2015)
32. Cuisinier, M.; Hart, C.; Balasubramanian, M.; Garsuch, A.; Nazar, L.F.: Radical or not radical: revisiting lithium–sulfur electrochemistry in nonaqueous electrolytes. Adv. Energy Mater. **5**, 1401801 (2015)
33. Cuisinier, M.; Cabelguen, P.-E.; Evers, S.; He, G.; Kolbeck, M.; Garsuch, A.; Bolin, T.; Balasubramanian, M.; Nazar, L.F.: Sulfur speciation in Li–S batteries determined by operando X-ray absorption spectroscopy. J. Phys. Chem. Lett. **4**, 3227–3232 (2013)
34. Yu, X.; Pan, H.; Zhou, Y.; Northrup, P.; Xiao, J.; Bak, S.; Liu, M.; Nam, K.W.; Qu, D.; Liu, J.: Direct observation of the redistribution of sulfur and polysulfides in Li–S batteries during the first cycle by in situ X-ray fluorescence microscopy. Adv. Energy Mater. **5**, 1500072 (2015)
35. Waluś, S.; Barchasz, C.; Bouchet, R.; Leprêtre, J.-C.; Colin, J.-F.; Martin, J.-F.; Elkaïm, E.; Baehtz, C.; Alloin, F.: Lithium/sulfur batteries upon cycling: structural modifications and species quantification by in situ and operando X-ray diffraction spectroscopy. Adv. Energy Mater. **5**, 1500165 (2015)
36. Nelson, J.; Misra, S.; Yang, Y.; Jackson, A.; Liu, Y.; Wang, H.; Dai, H.; Andrews, J.C.; Cui, Y.; Toney, M.F.: In operando X-ray diffraction and transmission X-ray microscopy of lithium sulfur batteries. J. Am. Chem. Soc. **134**, 6337–43 (2012)
37. Yang, Y.; Liu, X.; Dai, Z.; Yuan, F.; Bando, Y.; Golberg, D.; Wang, X.: In situ electrochemistry of rechargeable battery materials: status report and perspectives. Adv. Mater. **29**, 1606922 (2017)
38. Wolf, M.; May, B.M.; Cabana, J.: Visualization of electrochemical reactions in battery materials with X-ray microscopy and mapping. Chem. Mater. **29**, 3347–3362 (2017)
39. Lowe, M.A.; Gao, J.; Abruña, H.D.: Mechanistic insights into operational lithium–sulfur batteries by in situ X-ray diffraction and absorption spectroscopy. RSC Adv. **4**, 18347 (2014)
40. Kim, H.; Lee, J.T.; Magasinski, A.; Zhao, K.; Liu, Y.; Yushin, G.: In situ TEM observation of electrochemical lithiation of sulfur confined within inner cylindrical pores of carbon nanotubes. Adv. Energy Mater. **5**, 1501306 (2015)
41. Yang, Z.; Zhu, Z.; Ma, J.; Xiao, D.; Kui, X.; Yao, Y.; Yu, R.; Wei, X.; Gu, L.; Hu, Y.S.: Phase separation of Li_2S/S at nanoscale during electrochemical lithiation of the solid-state lithium–sulfur battery using in situ TEM. Adv. Energy Mater. **6**, 1600806 (2016)
42. Harks, P.P.R.M.L.; Mulder, F.M.; Notten, P.H.L.: In situ methods for Li–ion battery research: a review of recent developments. J. Power Sources **288**, 92–105 (2015)
43. Paolella, A.; Zhu, W.; Marceau, H.; Kim, C.-S.; Feng, Z.; Liu, D.; Gagnon, C.; Trottier, J.; Abdelbast, G.; Hovington, P.; Vijh, A.; Demopoulos, G.P.; Armand, M.; Zaghib, K.: Transient existence of crystalline lithium disulfide Li_2S_2 in a lithium–sulfur battery. J. Power Sources **325**, 641–645 (2016)
44. Lin, F.; Liu, Y.; Yu, X.; Cheng, L.; Singer, A.; Shpyrko, O.G.; Xin, H.L.; Tamura, N.; Tian, C.; Weng, T.C.; Yang, X.Q.; Meng,

Y.S.; Nordlund, D.; Yang, W.; Doeff, M.M.: Synchrotron X-ray analytical techniques for studying materials electrochemistry in rechargeable batteries. Chem. Rev. **117**, 13123 (2017)
45. Guo, J.: Synchrotron radiation, soft-X-ray spectroscopy and nanomaterials. Int. J. Nanotechnol. **1**, 193–225 (2004)
46. Bak, S.-M.; Shadike, Z.; Lin, R.; Yu, X.; Yang, X.-Q.: In situ/operando synchrotron-based X-ray techniques for lithium–ion battery research. NPG Asia Mater. **10**, 563–580 (2018)
47. Li, Q.; Qiao, R.; Wray, L.A.; Chen, J.; Zhuo, Z.; Chen, Y.; Yan, S.; Pan, F.; Hussain, Z.; Yang, W.: Quantitative probe of the transition metal redox in battery electrodes through soft X-ray absorption spectroscopy. J Phys. D Appl. Phys. **49**, 413003 (2016)
48. Zhang, L.; Ji, L.; Glans, P.A.; Zhang, Y.; Zhu, J.; Guo, J.: Electronic structure and chemical bonding of a graphene oxide–sulfur nanocomposite for use in superior performance lithium–sulfur cells. Phys. Chem. Chem. Phys. **14**, 13670–5 (2012)
49. Ji, L.; Rao, M.; Zheng, H.; Zhang, L.; Li, Y.; Duan, W.; Guo, J.; Cairns, E.J.; Zhang, Y.: Graphene oxide as a sulfur immobilizer in high performance lithium/sulfur cells. J. Am. Chem. Soc. **133**, 18522–5 (2011)
50. Wang, H.; Butorin, S.M.; Young, A.T.; Guo, J.: Nickel oxidation states and spin states of bioinorganic complexes from nickel L-edge X-ray absorption and resonant inelastic X-ray scattering. J. Phys. Cem. C **117**, 24767–24772 (2013)
51. Wujcik, K.H.; Wang, D.R.; Pascal, T.A.; Prendergast, D.; Balsara, N.P.: In situ X-ray absorption spectroscopy studies of discharge reactions in a thick cathode of a lithium sulfur battery. J. Electrochem. Soc. **164**, A18–A27 (2017)
52. Zhao, Q.; Zheng, J.; Archer, L.: Interphases in lithium–sulfur batteries: toward deployable devices with competitive energy density and stability. ACS Energy Lett. **3**, 2104–2113 (2018)
53. Ould Ely, T.; Kamzabek, D.; Chakraborty, D.; Doherty, M.F.: Lithium–sulfur batteries: state of the art and future directions. ACS Appl. Mater. Int. **1**, 1783–1814 (2018)
54. Li, M.; Chen, Z.; Wu, T.; Lu, J.: Li_2S- or S-based lithium–ion batteries. Adv. Mater. **30**, 1801190 (2018)
55. Li, M.; Amirzadeh, Z.; De Marco, R.; Tan, X.F.; Whittaker, A.; Huang, X.; Wepf, R.; Knibbe, R.: In situ techniques for developing robust Li–S batteries. Small Methods **2**, 1800133 (2018)
56. Zou, Q.; Lu, Y.C.: Solvent-dictated lithium sulfur redox reactions: an operando UV–Vis spectroscopic study. J. Phys. Chem. Lett. **7**, 1518–25 (2016)
57. Vijayakumar, M.; Govind, N.; Walter, E.; Burton, S.D.; Shukla, A.; Devaraj, A.; Xiao, J.; Liu, J.; Wang, C.; Karim, A.; Thevuthasan, S.: Molecular structure and stability of dissolved lithium polysulfide species. Phys. Chem. Chem. Phys. **16**, 10923–32 (2014)
58. Barchasz, C.; Molton, F.; Duboc, C.; Lepretre, J.C.; Patoux, S.; Alloin, F.: Lithium/sulfur cell discharge mechanism: an original approach for intermediate species identification. Anal. Chem. **84**, 3973–80 (2012)
59. Sun, D.; Hwa, Y.; Shen, Y.; Huang, Y.; Cairns, E.J.: Li_2S nano spheres anchored to single-layered graphene as a high-performance cathode material for lithium/sulfur Cells. Nano Energy **26**, 524–532 (2016)
60. Nan, C.; Lin, Z.; Liao, H.; Song, M.K.; Li, Y.; Cairns, E.J.: Durable carbon-coated $Li_2(S)$ core-shell spheres for high performance lithium/sulfur cells. J. Am. Chem. Soc. **136**, 4659–63 (2014)
61. Cai, K.; Song, M.K.; Cairns, E.J.; Zhang, Y.: Nanostructured $Li_{(2)}S$–C composites as cathode material for high-energy lithium/sulfur batteries. Nano Lett. **12**, 6474–9 (2012)
62. Zhou, G.; Tian, H.; Jin, Y.; Tao, X.; Liu, B.; Zhang, R.; Seh, Z.W.; Zhuo, D.; Liu, Y.; Sun, J.; Zhao, J.; Zu, C.; Wu, D.S.; Zhang, Q.; Cui, Y.: Catalytic oxidation of Li_2S on the surface of metal sulfides for Li–S batteries. Proc. Natl. Acad. Sci. **114**, 840–845 (2017)
63. Zhou, G.; Sun, J.; Jin, Y.; Chen, W.; Zu, C.; Zhang, R.; Qiu, Y.; Zhao, J.; Zhuo, D.; Liu, Y.; Tao, X.; Liu, W.; Yan, K.; Lee, H.R.; Cui, Y.: Sulfiphilic nickel phosphosulfide enabled Li_2 S impregnation in 3D graphene cages for Li–S batteries. Adv. Mater. **29**, 1603366 (2017)
64. Wang, L.; Wang, Y.; Xia, Y.: A high performance lithium-ion sulfur battery based on a Li_2S cathode using a dual-phase electrolyte. Energy Environ. Sci. **8**, 1551–1558 (2015)
65. Yang, Y.; Zheng, G.; Misra, S.; Nelson, J.; Toney, M.F.; Cui, Y.: High-capacity micrometer-sized Li_2S particles as cathode materials for advanced rechargeable lithium–ion batteries. J. Am. Chem. Soc. **134**, 15387–94 (2012)
66. Hwa, Y.; Zhao, J.; Cairns, E.J.: Lithium sulfide (Li_2S)/graphene oxide nanospheres with conformal carbon coating as a high-rate, long-life cathode for Li/S cells. Nano Lett. **15**, 3479–86 (2015)
67. Qiu, Y.; Rong, G.; Yang, J.; Li, G.; Ma, S.; Wang, X.; Pan, Z.; Hou, Y.; Liu, M.; Ye, F.; Li, W.; Seh, Z.W.; Tao, X.; Yao, H.; Liu, N.; Zhang, R.; Zhou, G.; Wang, J.; Fan, S.; Cui, Y.; Zhang, Y.: Highly nitridated graphene-Li_2S cathodes with stable modulated cycles. Adv. Energy Mater. **5**, 1501369 (2015)
68. Son, Y.; Lee, J.-S.; Son, Y.; Jang, J.-H.; Cho, J.: Recent advances in lithium sulfide cathode materials and their use in lithium sulfur batteries. Adv. Energy Mater. **5**, 1500110 (2015)
69. Tan, G.; Xu, R.; Xing, Z.; Yuan, Y.; Lu, J.; Wen, J.; Liu, C.; Ma, L.; Zhan, C.; Liu, Q.; Wu, T.; Jian, Z.; Shahbazian-Yassar, R.; Ren, Y.; Miller, D.J.; Curtiss, L.A.; Ji, X.; Amine, K.: Burning lithium in CS_2 for high-performing compact Li_2S-graphene nanocapsules for Li–S batteries. Nature Energy **2**, 17090 (2017)
70. Ai, G.; Dai, Y.; Mao, W.; Zhao, H.; Fu, Y.; Song, X.; En, Y.; Battaglia, V.S.; Srinivasan, V.; Liu, G.: Biomimetic ant-nest electrode structures for high sulfur ratio lithium–sulfur batteries. Nano Lett. **16**, 5365–72 (2016)
71. Ai, G.; Dai, Y.; Ye, Y.; Mao, W.; Wang, Z.; Zhao, H.; Chen, Y.; Zhu, J.; Fu, Y.; Battaglia, V.; Guo, J.; Srinivasan, V.; Liu, G.: Investigation of surface effects through the application of the functional binders in lithium sulfur batteries. Nano Energy **16**, 28–37 (2015)
72. Li, H.; Yang, X.; Wang, X.; Liu, M.; Ye, F.; Wang, J.; Qiu, Y.; Li, W.; Zhang, Y.: Dense integration of graphene and sulfur through the soft approach for compact lithium/sulfur battery cathode. Nano Energy **12**, 468–475 (2015)
73. Wang, H.; Yang, Y.; Liang, Y.; Robinson, J.T.; Li, Y.; Jackson, A.; Cui, Y.; Dai, H.: Graphene-wrapped sulfur particles as a rechargeable lithium–sulfur battery cathode material with high capacity and cycling stability. Nano Lett. **11**, 2644–7 (2011)
74. Song, J.; Gordin, M.L.; Xu, T.; Chen, S.; Yu, Z.; Sohn, H.; Lu, J.; Ren, Y.; Duan, Y.; Wang, D.: Strong lithium polysulfide chemisorption on electroactive sites of nitrogen-doped carbon composites for high-performance lithium–sulfur battery cathodes. Angew. Chem. Int. Ed. **54**, 4325–9 (2015)
75. Li, W.; Zhang, Q.; Zheng, G.; Seh, Z.W.; Yao, H.; Cui, Y.: Understanding the role of different conductive polymers in improving the nanostructured sulfur cathode performance. Nano Lett. **13**, 5534–40 (2013)
76. Chen, W.; Qian, T.; Xiong, J.; Xu, N.; Liu, X.; Liu, J.; Zhou, J.; Shen, X.; Yang, T.; Chen, Y.; Yan, C.: A new type of multifunctional polar binder: toward practical application of high energy lithium sulfur batteries. Adv. Mater. **29**, 1605160 (2017)
77. Wang, J.; Yao, Z.; Monroe, C.W.; Yang, J.; Nuli, Y.: Carbonyl-β-cyclodextrin as a novel binder for sulfur composite cathodes in rechargeable lithium batteries. Adv. Funct. Mater. **23**, 1194–1201 (2013)
78. Milroy, C.; Manthiram, A.: An elastic, conductive, electroactive nanocomposite binder for flexible sulfur cathodes in lithium–sulfur batteries. Adv. Mater. **28**, 9744–9751 (2016)
79. Seh, Z.W.; Zhang, Q.; Li, W.; Zheng, G.; Yao, H.; Cui, Y.: Stable cycling of lithium sulfide cathodes through strong affinity with a bifunctional binder. Chem. Sci. **4**, 3673 (2013)

80. Chen, C.Y.; Peng, H.J.; Hou, T.Z.; Zhai, P.Y.; Li, B.Q.; Tang, C.; Zhu, W.; Huang, J.Q.; Zhang, Q.: A quinonoid-imine-enriched nanostructured polymer mediator for lithium–sulfur batteries. Adv. Mater. **29**, 1606802 (2017)
81. Li, G.; Ling, M.; Ye, Y.; Li, Z.; Guo, J.; Yao, Y.; Zhu, J.; Lin, Z.; Zhang, S.: Acacia senegal-inspired bifunctional binder for longevity of lithium–sulfur batteries. Adv. Energy Mater. **5**, 1500878 (2015)
82. Ling, M.; Zhang, L.; Zheng, T.; Feng, J.; Guo, J.; Mai, L.; Liu, G.: Nucleophilic substitution between polysulfides and binders unexpectedly stabilizing lithium sulfur battery. Nano Energy **38**, 82–90 (2017)
83. Zhang, L.; Ling, M.; Feng, J.; Liu, G.; Guo, J.: Effective electrostatic confinement of polysulfides in lithium/sulfur batteries by a functional binder. Nano Energy **40**, 559 (2017)
84. Aurbach, D.; Pollak, E.; Elazari, R.; Salitra, G.; Kelley, C.S.; Affinito, J.: On the surface chemical aspects of very high energy density rechargeable Li–sulfur batteries. J. Electrochem. Soc. **156**, A694 (2009)
85. Cheng, X.B.; Zhang, R.; Zhao, C.Z.; Wei, F.; Zhang, J.G.; Zhang, Q.: A review of solid electrolyte interphases on lithium metal anode. Adv. Sci. **3**, 1500213 (2016)
86. Zhang, S.S.; Read, J.A.: A new direction for the performance improvement of rechargeable lithium/sulfur batteries. J. Power Sources **200**, 77–82 (2012)
87. Liang, X.; Wen, Z.; Liu, Y.; Wu, M.; Jin, J.; Zhang, H.; Wu, X.: Improved cycling performances of lithium sulfur batteries with $LiNO_3$-modified electrolyte. J. Power Sources **196**, 9839–9843 (2011)
88. Zhang, S.S.: A new finding on the role of $LiNO_3$ in lithium–sulfur battery. J. Power Sources **322**, 99–105 (2016)
89. Zhang, S.S.: Effect of discharge cutoff voltage on reversibility of lithium/sulfur batteries with $LiNO_3$-contained electrolyte. J. Electrochem. Soc. **159**, A920–A923 (2012)
90. Zhang, S.S.: Role of $LiNO_3$ in rechargeable lithium/sulfur battery. Electrochim. Acta **70**, 344–348 (2012)
91. Xiong, S.; Xie, K.; Diao, Y.; Hong, X.: Characterization of the solid electrolyte interphase on lithium anode for preventing the shuttle mechanism in lithium–sulfur batteries. J. Power Sources **246**, 840–845 (2014)
92. Li, W.; Yao, H.; Yan, K.; Zheng, G.; Liang, Z.; Chiang, Y.M.; Cui, Y.: The synergetic effect of lithium polysulfide and lithium nitrate to prevent lithium dendrite growth. Nature Commun. **6**, 7436 (2015)
93. Xiong, S.; Xie, K.; Diao, Y.; Hong, X.: On the role of polysulfides for a stable solid electrolyte interphase on the lithium anode cycled in lithium–sulfur batteries. J. Power Sources **236**, 181–187 (2013)
94. Xiong, S.; Xie, K.; Diao, Y.; Hong, X.: Properties of surface film on lithium anode with $LiNO_3$ as lithium salt in electrolyte solution for lithium–sulfur batteries. Electrochim. Acta **83**, 78–86 (2012)
95. Zhao, C.-Z.; Cheng, X.-B.; Zhang, R.; Peng, H.-J.; Huang, J.-Q.; Ran, R.; Huang, Z.-H.; Wei, F.; Zhang, Q.: Li_2S_5-based ternary-salt electrolyte for robust lithium metal anode. Energy Storage Mater. **3**, 77–84 (2016)
96. Jozwiuk, A.; Berkes, B.B.; Weiß, T.; Sommer, H.; Janek, J.; Brezesinski, T.: The critical role of lithium nitrate in the gas evolution of lithium–sulfur batteries. Energy Environ. Sci. **9**, 2603–2608 (2016)
97. Yan, C.; Cheng, X.-B.; Zhao, C.-Z.; Huang, J.-Q.; Yang, S.-T.; Zhang, Q.: Lithium metal protection through in-situ formed solid electrolyte interphase in lithium–sulfur batteries: the role of polysulfides on lithium anode. J. Power Sources **327**, 212–220 (2016)
98. Eberhardt, W.: Synchrotron radiation: a continuing revolution in X-ray science-diffraction limited storage rings and beyond. J. Electron. Spectrosc. Relat. Phenom. **200**, 31–39 (2015)
99. Hettel, R.: DLSR design and plans: an international overview. J. Synchrotron Radiat. **21**, 843–55 (2014)